UCRL-JC-107388
PREPRINT

The Autoignition Chemistry of Paraffinic Fuels and Pro-Knock and Anti-Knock Additives: A Detailed Chemical Kinetic Study

Charles K. Westbrook and William J. Pitz
Lawrence Livermore National Laboratory
Livermore, CA

William R. Leppard
Fuels and Lubricants Department
General Motors Research Lab. - Warren, MI

This Paper Was Prepared for Presentation to
The 1991 SAE International Fuels & Lubricants
Meeting & Exposition - Inn on the Park
Toronto, Canada

Oct. 7-10, 1991

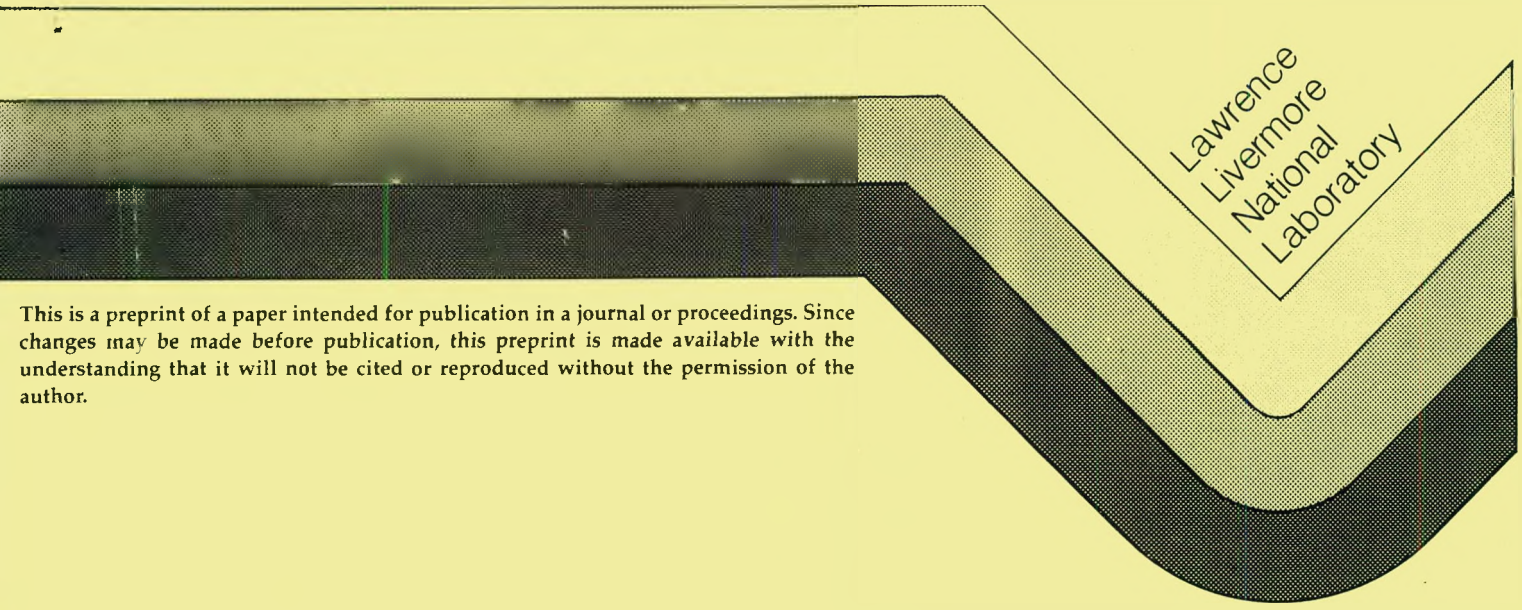

The Autoignition Chemistry of Paraffinic Fuels and Pro-Knock and Anti-Knock Additives: A Detailed Chemical Kinetic Study

UCRL-JC--107388

DE91 014992

Charles K. Westbrook and William J. Pitz
Lawrence Livermore National Laboratory
Livermore, California 94550

and

William R. Leppard
Fuels and Lubricants Department
General Motors Research Laboratories
Warren, Michigan 48090-9055

Abstract

A numerical model is used to examine the chemical kinetic processes which lead to knocking in spark-ignition internal combustion engines. The construction and validation of the model is described in detail, including the low temperature reaction paths involving alkylperoxy radical isomerization. The numerical model is then applied to C_1 to C_7 paraffinic hydrocarbon fuels, and a correlation is developed between the Research Octane Number (RON) and the computed time of ignition for each fuel. Octane number is shown to depend on the rates of OH radical production through isomerization reactions, and factors influencing the rate of isomerization such as fuel molecule size and structure are interpreted in terms of the kinetic model. The knock behavior of fuel mixtures is examined, and the manner in which pro-knock and anti-knock additives influence ignition is studied numerically. The kinetics of methyl tert-butyl ether (MTBE) is discussed in particular detail.

INTRODUCTION

Engine knock represents an important limit to the compression ratio at which an internal combustion engine can operate. Because engine efficiency and fuel economy are approximately proportional to compression ratio under normal operating conditions, the onset of engine knock therefore limits the efficiency of these engines. Suppression of knocking behavior in internal combustion engines would permit operation at higher compression ratios and higher operating efficiency than in current engines.

Suppression of knock can be achieved in several general ways. First, additional hydrocarbon and oxygenated blending stocks with higher knock resistance can be blended into the primary fuel, providing a fuel mixture with higher knock resistance. Alternatively, non-hydrocarbon additive compounds may be incorporated into the fuel, additives which act by kinetically retarding the autoignition process in the engine chamber. Heat transfer from the igniting gases to the combustion chamber walls can also retard the onset of engine knock, and fluid mechanics changes in the engine combustion chamber can also have a significant impact on the tendency of an engine to knock.

These factors influencing knocking tendency have been well understood on a qualitative and semi-quantitative basis for many years [1]. The use of octane ratings, especially research octane number (RON), motored octane number (MON), and blending octane number has been established to provide guidance for comparing the knocking tendency of most fuels of interest to

automotive combustion. However, it is widely recognized [2] that the octane number of mixtures of different fuels, even those mixtures consisting of only two constituents, cannot be predicted with the precision necessary for practical applications. Similar prediction for arbitrary mixtures of many different fuel species represents an even more difficult problem with immense economic implications for both the petroleum and automotive industries.

The present work is part of a long-term study of the fundamental chemical factors which control the tendency of hydrocarbon fuels to knock in internal combustion engines. Previous kinetic modeling studies [3-12] have gradually and systematically built the detailed reaction mechanisms necessary for the present work. These have included high temperature shock tube problems, intermediate temperature flow reactor models, and lower temperature static reactor and stirred reactor models, each of which emphasizes different families of elementary reactions with much different dependencies on temperature, pressure, and fuel-oxidizer concentrations. In the present paper, these different elements are combined in order to address the uniquely difficult kinetic problem of engine knock, which encompasses all of the ranges of temperature and pressure encountered in the above types of problems.

TRENDS FOR KNOCK TENDENCY

For single-component paraffinic fuels, several general trends relating fuel structure with octane number are evident. First, for fuels with the same overall structure, octane number decreases steadily as the size of the fuel molecule increases. This can be illustrated for two families of fuels, the straight-chain n-alkanes and the branched 2-methyl alkanes from propane to heptane, using RON values for illustration.

n-alkane	RON	2-methyl alkane	RON
propane	112	2-methyl propane	102
n-butane	94	2-methyl butane	92
n-pentane	62	2-methyl pentane	73
n-hexane	25	2-methyl hexane	42
n-heptane	0	2-methyl heptane	22

The second major structural factor affecting octane number is the number of side branches on the molecule. For a given total number of carbon atoms in the hydrocarbon fuel molecule, the octane number increases dramatically as the number of methyl side groups increases. This is illustrated in Fig. 1 for the isomers of hexane. The same trend is observed for the nine structural isomers of heptane shown below.

heptane	RON
n-heptane	0
2-methyl hexane	42
3-methyl hexane	52
3-ethyl pentane	65
3,3-dimethyl pentane	81
2,4-dimethyl pentane	83
2,3-dimethyl pentane	91
2,2-dimethyl pentane	93
2,2,3-trimethyl butane	112

1) n-hexane — Octane no. = 25

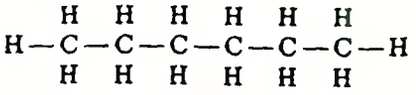

2) 2-methyl pentane — Octane no. = 73

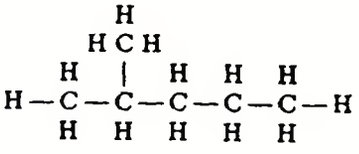

3) 3-methyl pentane — Octane no. = 74

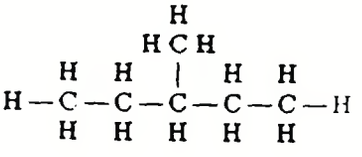

4) 2-2-dimethyl butane — Octane no. = 92

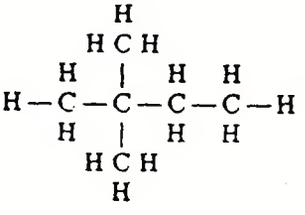

5) 2-3-dimethyl butane — Octane no. = 99

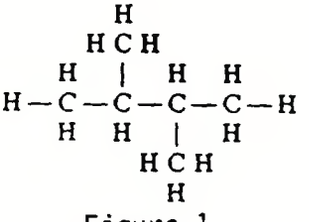

Figure 1

Isomers of hexane and their values for Research Octane Number (RON)

For both hexane and heptane, the addition of each methyl side chain produces a large increase in octane number. For the last of the heptane isomers listed above, there are three side methyl groups and the RON value is extremely high. Another distinct feature for heptane is the occurrence of an isomer with a side ethyl chain. Comparison of this species with 2-methyl pentane from Fig. 1 shows that addition of a side ethyl chain to n-pentane does not increase its octane rating as dramatically as the addition of a side methyl chain.

A truly useful theoretical model for prediction of knocking tendency must be able to reproduce the above trends for the variability of octane number with changes in fuel size and structure. It must also provide an explanation of these trends in fundamental chemical terms. Only then is it possible or realistic to use such a model to investigate the more complex problems of the behavior of mixtures of fuels and the use of additives to modify knock tendency. In the next section of this paper, we will describe how the chemical kinetic model is constructed. The following section will then demonstrate the overall validation of the model through applications to a considerable range of fuel molecules, including all of the alkane isomers from methane to hexane and most of the isomers of heptane. Finally, the influences of a range of additive compounds will be addressed. Both pro-knock and anti-knock additives will be studied numerically, with particular emphasis on the prominent antiknock species methyl tert-butyl ether (MTBE) and ethyl tert-butyl ether (ETBE). In each case, the chemical kinetic factors responsible for the observed behavior will be examined.

CHEMICAL KINETIC REACTION MECHANISMS

As already noted, engine knock is a particularly demanding problem for kinetic modeling because the reacting gases experience such a wide range of temperature and pressure during its history. Following their induction into the combustion chamber at approximately room temperature and atmospheric pressure, these gases are steadily compressed, first by the motion of the piston and then by the propagation of the flame front. The end gases, those reactants which are the last to be consumed by the flame front, are reacting homogeneously during all of this time, which can be as long as 50 milliseconds or more in a low-speed engine. Given enough time, these end gases will ignite spontaneously. Under normal, non-knocking conditions, the end gases are consumed by the flame front before they complete their ignition. However, if the end gases react rapidly, they can ignite prior to the arrival of the flame front, and their energy release will produce the acoustic pressure oscillations in the engine that we associate with knocking behavior.

Modifications to the composition of the end gases which accelerate their ignition will therefore promote knocking behavior, while changes which slow this ignition will discourage knock. Furthermore, since flame propagation in engine combustion chambers is relatively insensitive to factors such as fuel molecule size and structure, the knock tendency of different fuels can be ranked by comparing their relative rates of thermal ignition; if one fuel molecule ignites faster than another, its octane rating will generally be lower.

As a result of these factors, we interpret the problem of numerical prediction of knock tendency as one of computing accurately the time of thermal autoignition of the end gas, under the conditions of temperature and pressure appropriate to a particular engine and operating conditions. We have devoted particular attention to the low speed, 600 rpm CFR engine cycle which is used experimentally to determine research octane number (RON), primarily because this provides a quantitative basis for comparisons of different fuels. However, the general principles involved do not depend on the engine speed or other specific engine conditions.

General Features of Hydrocarbon Fuel Oxidation

The overall process of hydrocarbon fuel combustion consists of converting the fuel and oxidizer to water and carbon dioxide. This is done by gradually disassembling the fuel into smaller pieces, which are then sequentially consumed to produce final products. Modeling of this process has been discussed in detail [13-15], and this material will be summarized briefly here, since it forms the basis for the knock model used in all of our calculations. Perhaps the most interesting feature of engine knock kinetics is the fact that the chain branching reactions change as the end gas temperature increases during the engine cycle.

Chain Initiation

Initiation reactions for these paraffinic fuels consist of thermal decomposition of the fuel into smaller fragments, indicated by

$$\text{Fuel} = R_1 + R_2$$

where R refers to a radical (usually an alkyl radical), as well as reactions between fuel molecules and molecular oxygen, given by

$$\text{Fuel} + O_2 = R + HO_2 \quad .$$

These reactions are important in generating an initial radical pool. The thermal dissocation reaction has a high activation energy and is therefore not important at the temperatures of typical end gases early in the engine cycle. Therefore, hydrogen abstraction from the fuel by molecular oxygen is the dominant initiation reaction. In terms of contribution to the overall time to ignition, these initiation reactions are usually of minor importance since they consume little of the fuel. Their importance is in creating a radical pool, and after this is accomplished, other reactions become much more significant.

Abstraction of H atoms

Following the initiation phase of ignition, the most important series of reactions removes H atoms from the fuel molecule. Virtually all of this process occurs through reactions with radical species which abstract single H atoms, producing alkyl radicals and another small product species. In our current models, these attacking species include OH, H, O, CH_3, HO_2, CH_3O, O_2, C_2H_5, C_2H_3, and CH_3O_2. Primary C - H bonds are stronger than secondary bonds, which are in turn stronger than tertiary bonds. Since very few site-specific H atom abstraction reactions have been studied experimentally for larger hydrocarbon fuel molecules, it is necessary to estimate those reaction rates in some realistic way. This has been done by assuming that, for each radical reactant, abstraction of H atoms at each primary site is approximately equal to the rate of primary H atom abstraction in some model hydrocarbon fuel species. Similarly, the rate of secondary H atom abstraction is equal, per H atom site, to the observed rate in fuels where the actual rate has been measured, and correspondingly for tertiary bonds.

Radical	Site	Rate per H atom	Rate at 850K
H	primary	$9.3\times10^{6}T^{2}\exp(-7700/RT)$	7.04×10^{10}
	secondary	$4.5\times10^{6}T^{2}\exp(-5000/RT)$	1.68×10^{11}
	tertiary	$1.26\times10^{14}\exp(-7300/RT)$	1.67×10^{12}
OH	primary	$1.7\times10^{9}T^{0.97}\exp(-1590/RT)$	4.60×10^{11}
	secondary	$2.3\times10^{7}T^{1.61}\exp(-40/RT)$	1.18×10^{12}
	tertiary	$5.7\times10^{10}T^{0.51}\exp(-63/RT)$	1.71×10^{12}
O	primary	$7.3\times10^{5}T^{2.4}\exp(-5500/RT)$	3.02×10^{11}
	secondary	$2.4\times10^{5}T^{2.5}\exp(-2230/RT)$	1.35×10^{12}
	tertiary	$1.1\times10^{13}\exp(-3280/RT)$	1.58×10^{12}
HO_2	primary	$1.3\times10^{12}\exp(-19400/RT)$	1.33×10^{07}
	secondary	$1.2\times10^{12}\exp(-17000/RT)$	5.10×10^{07}
	tertiary	$2.2\times10^{12}\exp(-14400/RT)$	4.36×10^{08}
CH_3	primary	$2.1\times10^{11}\exp(-11600/RT)$	2.18×10^{08}
	secondary	$2.0\times10^{11}\exp(-9500/RT)$	7.21×10^{08}
	tertiary	$1.0\times10^{11}\exp(-7900/RT)$	9.30×10^{08}
O_2	primary	$4.2\times10^{12}\exp(-49000/RT)$	1.06×10^{00}
	secondary	$1.0\times10^{13}\exp(-47600/RT)$	5.76×10^{00}
	tertiary	$2.0\times10^{13}\exp(-41300/RT)$	4.80×10^{02}
CH_3O	primary	$5.3\times10^{10}\exp(-7000/RT)$	8.40×10^{08}
	secondary	$5.5\times10^{10}\exp(-5000/RT)$	2.85×10^{09}
	tertiary	$1.9\times10^{10}\exp(-2800/RT)$	3.62×10^{09}
CH_3O_2	primary	$2.0\times10^{12}\exp(-20430/RT)$	1.12×10^{07}
	secondary	$2.0\times10^{12}\exp(-17700/RT)$	5.62×10^{07}
	tertiary	$2.0\times10^{12}\exp(-14000/RT)$	5.02×10^{08}

Table I

Rates of major H atom abstraction reactions

Rates per H atom site, units are cm-mol-cal-sec

Rates of H atom abstraction per H atom site used in the present computational analysis are tabulated in Table I. For each fuel molecule, this rate must be multiplied by the number of available H atoms at each type of site. Experimental data for any of these fuels would be used to refine the rate data, but at the present time no such data are available.

Second, logically different H atom sites in each fuel molecule must be distinguished, since each product path leads to a different group of products and a distinctive impact on the overall chain branching nature of the reaction mechanism. This point has been made in studies of higher temperature ignition [3,12], where different alkyl radicals lead to different rates of H atom production, but the same distinction with respect to lower temperature oxidation reactions has not previously been made. Still, as the following discussion will demonstrate, the same distinctions are very important, indeed essential, in determining the overall rates of ignition.

Perhaps the most important H atom abstraction reaction under end-gas ignition conditions (and also under nearly all hydrocarbon oxidation conditions, regardless of combustion environment) is the reaction with OH

$$\text{Fuel} + \text{OH} = \text{R} + \text{H}_2\text{O} \quad .$$

Throughout the end gas history, these reactions with OH consume the greatest fraction of the fuel. For this reason, one of the keys to calculating the time of ignition is to be able to correctly predict the levels of OH radicals. At lower temperatures, there are several reaction paths which lead to the production of OH in substantial quantities; as our model calculations will show in the following discussions, some of

these reaction paths depend very strongly on the size and structure of the fuel molecule, the same factors which are known empirically to have strong influences on engine knock. For end gas conditions, the HO_2 radical is also of particular importance, and the abstraction reaction

$$\text{Fuel} + HO_2 = R + H_2O_2$$

also plays a very important role, since the H_2O_2 produced then decomposes to produce OH radicals via

$$H_2O_2 + M = OH + OH + M \quad ,$$

where M is any third body involved in the reaction. In addition to its production of OH radicals, this series of reactions is important because it consumes one radical (HO_2) and produces three radical species, R + OH + OH, leading to a great deal of chain branching. This sequence is responsible for the actual end gas ignition that produces knock and becomes effective at temperatures sufficiently high to decompose H_2O_2 at a significant rate. Under typical end-gas conditions this occurs at a temperature slightly above 900K.

Alkylperoxy isomerization

At temperatures above 1000K, the alkyl radicals that are produced by H atom abstraction from the fuel decompose readily into smaller fragment species. However, end-gas autoignition and all of the chemical activity that leads to it occur at temperatures between about 500K and 950K. At these lower temperatures, the activation energies for alkyl radical decomposition are too high for these reactions to occur at any significant rate. Instead, most of the alkyl radicals react through addition of molecular oxygen to produce alkylperoxy radicals RO_2,

$$R + O_2 = RO_2 \quad .$$

Our calculations have shown that the subsequent reactions of these RO_2 radicals are responsible for most of the observed variations in knock tendency with fuel molecular structure and size.

There are three principal reaction paths for the RO_2 radicals:

a) The radical can dissociate back to its original reactants, $R+O_2$. This establishes an equilibrium between R and RO_2 which changes rapidly with temperature. At sufficiently high temperatures, above about 900K under our present conditions, RO_2 decomposition becomes so rapid that there is not enough RO_2 for the other reaction paths of RO_2 (discussed below) to proceed. This decomposition is also responsible for the negative temperature coefficient of reaction that is observed in hydrocarbon oxidation in certain other environments, and the temperature above which the equilibrium concentration of RO_2 is less than that of R is often termed the "ceiling temperature" [16].

b) The RO_2 radical can abstract H atoms from other species, most often from the fuel molecules, producing an alkylhydroperoxide ROOH. This will then decompose by breaking the O - O bond, producing OH radicals and an oxygenated radical which decomposes further to make at least one additional radical species. This sequence is strongly branching, regenerating the alkyl radical plus at least two additional radicals, including OH.

c) The alkylperoxy radical can abstract an H atom from another location in the radical itself. The majority of the resulting modified radical products then decompose to yield an OH radical and a relatively stable epoxide species. There are two major considerations which control the rate of this internal H atom abstraction. The first issue is the type of

site from which the H atom is abstracted. That is, the energy barrier to primary H atom abstraction is greater than that for secondary abstraction, and abstraction of tertiary H atoms is easier than either primary or secondary. The second factor of importance is the distance between the O - O radical site and the H atom to be abstracted. This factor is termed the ring strain energy and reflects the fact that this type of abstraction of H atoms proceeds through a ring-like transition state in which the O - O radical site must physically approach the H atom site. There is an energy barrier to this approach which varies with the number of atoms in the ring-like transition state. The smallest such transition state ring consists of five atoms, including the H atom, and has the highest energy barrier against its formation. As the ring size increases, the energy barrier decreases, reaching a minimum value when the ring consists of six or seven atoms and increasing slightly for larger ring-like states.

Therefore, for each internal H atom abstraction reaction, the overall activation energy of that reaction is a combination of the ring strain energy and the energy barrier for abstraction at the particular type of site (i.e. primary, secondary or tertiary). The principles involved can be illustrated using 2-methyl pentane as an example

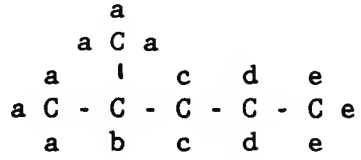

where the lower case letters a,b,c,d and e indicate logically distinct H atoms. Those labeled 'a' and 'e' are located at primary sites, 'b' is located at a tertiary site, and the 'c' and 'd' H atoms are at secondary sites. If one of the 'd' H atoms is removed by reaction with some type of

radical, the product alkyl radical can be indicated as

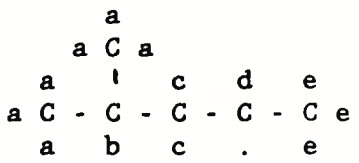

Following addition of molecular oxygen at the now-vacant 'd' site, the product alkylperoxy radical is given as

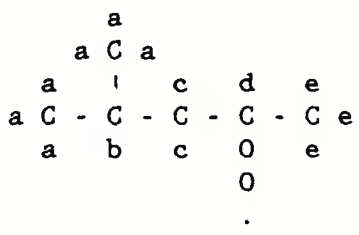

Following the discussion above, this radical can then abstract any of the remaining H atoms within the radical species, creating a O - O - H group and leaving an unoccupied site. In the above RO_2 radical, the ring strain energy barriers are greatest for the 'c' and 'e' H atoms, since they are at sites immediately next to the site of the O - O group. Internal abstraction of a 'c' H atom would proceed more rapidly than for an 'e' H atom because, while both involve the same ring strain energy barrier, the 'e' H atoms are bound at primary sites while the 'c' H atoms are bound at secondary sites and are thus more easily abstracted.

Furthermore, the trade-off between ring strain energy and the type of site can be illustrated by comparing the internal abstraction above of the 'a' and 'b' H atoms. The ring strain contribution to the rate expression is actually greater for the 'b' H atom (6 atoms in the transition state ring) than for the 'a' H atoms (7 atoms in the ring), but there is a much larger difference between a primary and tertiary C - H bond, with the result that the overall activation energy for abstracting the 'b' H atom is significantly smaller than for the 'a' H atoms. Thus the fastest internal abstraction site in the above RO_2 radical is from the 'b' site.

We can use the same type of reasoning to examine the internal H atom abstraction paths in the case of iso-octane, with its high octane number of 100 (the RON for the above fuel, 2-methyl pentane, is equal to 73). In iso-octane, the most easily abstracted H atom is located at the single tertiary site. For illustration, if we assume that this tertiary H atom has been abstracted and an O_2 molecule has been added at this location, the resulting RO_2 radical can be indicated schematically as

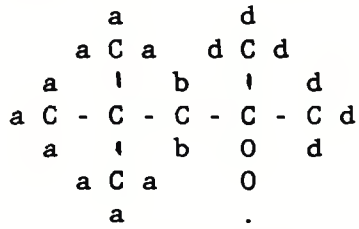

If we now look for the possible paths for internal abstraction of H atoms, it becomes clear that none of the remaining H atoms can easily be abstracted by the O - O site. The six 'd' H atoms have a double penalty because they have the maximum possible ring strain energy (i.e. 5 atoms in the ring) and are also located at primary sites. The nine 'a' H atoms incur a minimal ring strain energy barrier, since they involve a 7 atom transitional ring structure. However, these are all located at primary sites and pay a significant penalty in terms of activation energy. Finally, the two 'b' H atoms are located at secondary sites, which makes them easier to abstract, but they incur a substantial ring strain energy barrier because they involve a strained 5 atom transition state ring. In summary for this RO_2 radical, there are no easily abstracted H atoms which do not involve significant ring strain or primary site activation energy barriers, so the rates of these processes are all relatively small.

In Table II, the rates of internal H atom abstraction are summarized as functions of the type of H atom abstracted and the size of the intermediate ring involved. These rates are applicable for each H atom at the relevant location, so in the above example for iso-octane, internal abstraction of 'a' H atoms (with 9 such 'a' H atoms accessible) will have a rate expression of $4.59 \times 10^{11} \exp(-25100/RT)$ sec^{-1}. This is a 7 atom transition state ring, involving H atoms bonded at a primary site. From Table II, this rate is found by combining 9 times the A factor per H atom of 5.1×10^{10} and the activation energy of 25100 cal/mol. The variations in these quantities with ring size and the type of site clearly show the energy barriers that discourage reactions with highly strained rings and primary H atoms.

These are the values for the rate expressions used in the present model calculations. It should be noted that the experimental and theoretical bases for these values are very weak; even in the one case that has been studied at length in recent publications [17-20], where the alkyl radical involved is the ethyl radical C_2H_5, there are serious differences in the rate parameters resulting from the analyses. As a result, in view of the importance of these rate parameters in our computed models, there is a great need for further studies to refine our knowledge of RO_2 isomerization reactions.

Type of site	Atoms in transition state ring	Reaction Rate log A	E_a	Rate at 850K
primary	5	11.45	30000	5.44×10^3
primary	6	11.08	27000	1.37×10^4
primary	7	10.71	25100	1.80×10^4
primary	8	10.48	26000	6.23×10^3
secondary	5	11.05	26500	1.72×10^4
secondary	6	11.26	23400	1.75×10^5
secondary	7	11.48	21500	8.94×10^5
secondary	8	11.48	23000	3.68×10^5
tertiary	5	11.78	23000	7.34×10^5
tertiary	6	11.48	20100	2.05×10^6
tertiary	7	11.48	17900	7.54×10^6
tertiary	8	11.48	19000	3.93×10^6

Table II

Rates of Alkylperoxy Radical Isomerization Reactions
Activation energies are in cal/mol
Rates are in sec^{-1}

A final comment regarding RO_2 processes in iso-octane can be made. In the above examples it was assumed that the initial H atom abstraction from iso-octane had taken place at the tertiary site. If we assume instead that one of the secondary H atoms had been abstracted, followed by O_2 addition, all of the above analysis leads to exactly the same result, that there are no H atoms easily abstracted within the RO_2 radical. If we then carry out the same analysis for any of the primary H atom sites in iso-octane, we find that internal abstraction is appreciable from either the secondary or tertiary sites in the RO_2, so these reactions will proceed quite rapidly. However, because the 'a' and 'd' H atoms in the iso-octane fuel molecule are located at primary sites, they are relatively difficult to abstract. Once abstracted, the O_2 addition and RO_2 isomerization reactions proceed rapidly, but relatively few such primary-site alkyl radicals are produced to begin these paths. Overall, the conclusion of this analysis is that very little RO_2 isomerization should be observed when iso-octane is the fuel, a result which is consistent with experimental observations [21], and with the high octane number of iso-octane.

We can repeat the same type of analysis for the other primary reference fuel, n-heptane. There are no tertiary H atoms in n-heptane, so we assume that the initial H atom abstraction would take place preferentially at one of the secondary sites. Followed by O_2 addition, this can lead to the RO_2 radical

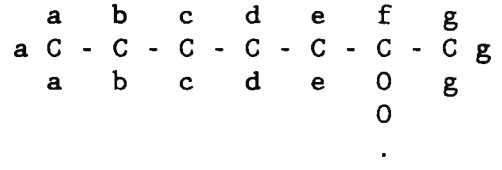

The 'b' and 'c' H atoms, located at secondary sites and involving transition state ring structures of seven and eight atoms, are very easily abstracted internally, so the rate of RO_2 isomerization is rapid. The same conclusion can be obtained for any of the other secondary sites in n-heptane. The overall conclusion is that there are ample opportunities for internal H atom abstraction reactions in the n-heptane RO_2 system. These paths lead to significant amounts of OH production, rapid reaction of n-heptane and a distinct tendency of n-heptane to ignite and knock. In addition, in contrast with the case for iso-octane, the product species from RO_2 isomerization in n-heptane are observed experimentally in large quantities [22].

An important conclusion of our modeling work, to which we will return below in our discussions of the computed results for a wide range of hydrocarbon fuels, is that production of OH through these RO_2 isomerization reactions is a central factor which influences knock tendency. Fuels for which these paths involve large ring strain energy barriers and large fractions of primary C - H bonds do not produce large numbers of OH radicals through these paths, do not ignite easily and are observed to have high octane numbers.

As we noted briefly above, subsequent to internal abstraction of H atoms within the RO_2 radical, the product usually decomposes leading to OH radicals and an epoxide species. For example, again using 2-methyl pentane for illustration, we can indicate the product of one possible RO_2 isomerization reaction by

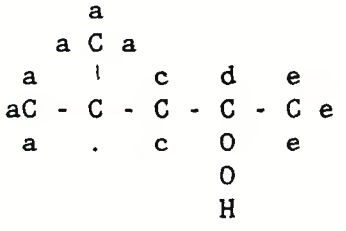

where the 'b' H atom was abstracted. The principal decomposition path for this radical is for the O - O bond to break, leaving an OH radical and a complex radical that proceeds to connect the two unbonded sites into a cyclic ether. In the above example the cyclic ether includes a ring with three C atoms and one O atom and is therefore the compound 2,2,4-trimethyl oxetane. Our current model includes cyclic ethers with one O atom and anywhere from 2 to 5 C atoms in this ring structure. Similar to the case for the ring strain energy associated with internal abstraction of the H atom discussed above, there is an analogous energy barrier to cyclization and OH production that is dependent on the ring size. Following the recommendations of Pollard [23], we assume that this energy barrier has the values listed in Table III.

Number of C atoms in ring	Energy barrier (cal)	Cyclic ether produced
2	14000	oxiran
3	13000	oxetan
4	3000	tetrahydrofuran
5	0	tetrahydropyran

Table III
Energy barriers in cal/mol for cyclization of QOOH species

The rates of cyclization in these compounds are not well established by experimental data, and just as in the case of the RO_2 internal H atom abstraction reactions, work is needed to refine this portion of these reaction mechanisms.

A special case can occur when the H atom is internally abstracted at the ß - site, that is, from the C atom located two carbon atoms away from the O - O site. Following the breaking of the O - O bond, it is also possible for the resulting radical species to decompose via ß - scission, yielding a carbonyl and an alkene species.

One special case for QOOH species decomposition occurs when the RO_2 radical abstracts a H atom immediately adjacent to the O - O site. This situation, indicated schematically by

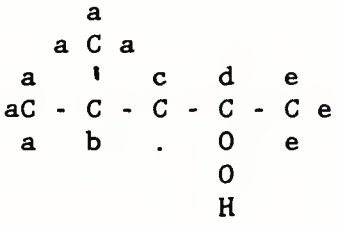

results in two possible decomposition paths being available. One already discussed above involves the formation of an oxiran and an OH radical by breaking the O - O bond. However, another alternative, with a generally faster rate at end-gas temperatures, involves breaking the C - O bond above, yielding HO_2 and an olefin product. Partly because of the lesser reactivity of the HO_2 radical relative to the OH radical produced by breaking the O - O bond, and partly due to the greater stability of the olefin relative to the cyclic ether, this second HO_2 path tends to retard the rate of ignition while breaking the O - O bond and producing OH tends to accelerate the ignition process. Our computed results for ignition are rather sensitive to the relative rates of these two paths for decomposition of this subset of the QOOH radicals.

A final reaction path for QOOH consists of addition of a second O_2 molecule, followed by another internal H atom abstraction. In our model, these paths eventually produce two OH radicals and small radical and stable species. However, there is very little experimental information on these reaction paths, and much of our treatment of these reactions is very speculative.

The reaction mechanisms for the subsequent oxidation of the large cyclic ethers and the large olefins produced in the above reaction paths are also not very well established. For the olefins, we have some guidance based on experience and experimental results for much smaller olefins such as ethylene, propene, and isobutene. However, the applicability of this experience and appropriate reaction rate expressions to larger olefins is not particularly well known. Similarly, the elementary reactions consuming the many cyclic ethers which are included, and rate expressions and product distributions for those reactions have not been studied experimentally except for the few small species such as ethylene oxide and propene oxide. Even for these few species there is very little available kinetic data. As a result, we are forced to make some rather broad assumptions regarding reaction paths and rate expressions. For the most part, we assume that these species are consumed by radical attack, especially by OH and HO_2, the radicals which have the greatest concentrations under end gas ignition conditions. We assume that these abstractions proceed at rates approximately equal to their rates in alkanes of comparable size and structure, and the resulting radical species then decompose into smaller fragments for which the model possesses better kinetic information.

Clearly, this is another submechanism which needs further attention by experimental studies. However, our calculations have shown very little sensitivity to variations in the rates and product distributions of these large olefin and cyclic ether reactions. As a result, we have felt justified in making these simplifying assumptions and proceeding, although better kinetic data in these areas would increase confidence in the computed results from the model.

For thermochemical data of many large hydrocarbon species, both stable and radical compounds, we have used standard thermochemical means of estimating values which are not available from experiments. Heats of formation and specific heat data of the stable species are generally known, and specific heats of radical species are estimated. These estimates do not involve significant errors, primarily because these species are present in such small quantities. Heats of formation for large hydrocarbon radicals are estimated using bond additivity arguments with acceptable precision. Because our numerical model [24] prescribes both forward and reverse reaction rates, it is less sensitive to errors in thermochemical data than other models which compute the reverse reaction rates from thermochemical data. For reactions involving large hydrocarbon species, both forward and reverse reaction rates are specified.

The reaction mechanisms for the smaller species, including C_4 species and smaller, are based on development which has been carried out over many years [3]. Of particular concern has been the testing of the portions of the reaction mechanism which relate to hydrocarbon oxidation at temperatures between about 500K and 900K, where most of the knock chemistry occurs. For this range of conditions, the model has been tested for static and stirred reactor data [8,11] and generally excellent results have been obtained.

KNOCK MODELING

Our detailed reaction mechanisms are first tested and validated by comparisons between computed and experimental results in simplified or idealized combustion environments. These include shock tubes, flow reactors, and laminar flames, where the boundary and initial conditions are well defined and the physical conditions for the combustion are very simple. Finally, the reaction mechanism is ready to use in an engine simulation.

We have attempted to reproduce end-gas conditions as closely as possible in our calculations. As already noted, the end gases in the engine chamber are subjected to a temperature and pressure history that is the result of piston motion, flame propagation through the combustion chamber, and heat transfer between the end gases and the engine chamber walls. The chemical kinetic model that we wish to use describes the reactions of the end gas under these conditions. However, the model does not attempt to describe all of the flame propagation, complex geometry, and other phenomena in the actual engine. Instead, the model is able to simulate all of these external phenomena only insofar as they influence the temperature and pressure history of the end gas. The resulting numerical model therefore consists of only one spatial zone, with the boundary conditions of pressure and temperature incorporated implicitly. The effects of heat transfer between the end gas and the engine combustion chamber walls are incorporated into a single heat transfer coefficient, with the heat transfer rate then proportional to the temperature difference between the end gas and the problem boundary corresponding to the combustion chamber wall.

Experimental pressure-time values were measured in a CFR engine with the compression ratio and operating conditions set at the values corresponding to a RON of 90. Under these conditions, knock is therefore not observed if the RON of the fuel is higher than 90, while knock occurs if the RON of the fuel is less than 90. For the measurements, iso-octane was used in order to prevent knock from distorting the measured pressures. Furthermore, when knock occurs, it typically appears at about 22° after TDC. This indicates that the last portion of end gas in this engine is consumed by the flame front at approximately 22° after TDC. We assume that the rate of flame propagation does not change appreciably as the octane number of the fuel is varied, so the onset of knock is attributed to changes in the rate of thermal ignition of the end gas. In terms of reaction kinetics, fuels with RON greater than 90 ignite relatively slowly and have not completed this process by the time they are consumed by the flame. In contrast, fuels with RON less than 90 react more rapidly and ignite spontaneously before the flame arrives, resulting in knocking behavior.

Computationally, we apply exactly the same reasoning as in the experimental approach. The computational end gas is subjected to the same pressure history as that measured in the engine at the 90 RON conditions. With a Primary Reference Fuel (PRF) mixture of 90% iso-octane and 10% n-heptane (i.e. RON=90), we then used the numerical model to compute the time of ignition of this mixture. The time of ignition was found to depend on the value chosen for the heat transfer coefficient, so this coefficient was calibrated such that this RON 90 mixture ignited very shortly after the above time of 22° after TDC. This model calibration was then retained without further change throughout the subsequent series of computations.

With this same pressure-time history and heat transfer coefficient, the model then integrates kinetic rate equations for the fuel being used, together with its intermediate products and all other species which can contribute to its ignition. For the larger fuel molecules included in this project, these reaction mechanisms can become enormous, with as many as 500 different chemical species and 2500 elementary chemical reactions. By comparison with a typical methane oxidation mechanism with perhaps 30 chemical species and 100 elementary reactions, these mechanisms are very large. They also require substantial amounts of computer time to calculate the ignition times, as much as 30 minutes of CRAY supercomputer time for a single case. The same calculations can be carried out on current minicomputers but require correspondingly longer execution times.

With this modeling approach, we then expect that the computed time of thermal end gas ignition will vary with the RON of the particular fuel mixture being studied. The simplest expectation is that when the model indicates end gas ignition earlier than 22° ATDC, this is equivalent to a numerical prediction that the RON of that mixture is less than 90. When the computed time of ignition is later than 22° ATDC or that the end gas does not ignite at all, the model is indicating that the RON of that fuel is greater than 90. This procedure could be repeated computationally using pressure-time histories for other values of RON to provide a computational analog to the actual test procedure used experimentally.

However, in the present study we have used a somewhat simplified approach, using only the RON 90 pressure history, selected because it is close to the value of RON found in conventional automotive fuels and reasonably close to the RON values of many of the fuels we have studied computationally. With this single pressure history, we then use relative

times of autoignition to compare RON values of different compounds and fuel mixtures. That is, if the computed time of ignition for one fuel is earlier than that for a second fuel, then the model is indicating that the RON of the first fuel is less than the RON of the second. In this way we can develop a continuous correlation between the computed time of autoignition and the RON of the fuel. In the following section we will show how successful this approach has been for single-component fuels. In a later section we will show how pro-knock additives shorten the ignition time for a given hydrocarbon fuel and anti-knock additives lengthen the time to achieve ignition.

KNOCKING TENDENCIES OF SINGLE-COMPONENT FUELS

All of the alkane hydrocarbons from ethane through hexane, including all isomeric forms, were studied numerically. In addition, seven of the nine isomers of heptane, as well as iso-octane were included. In all of these computed models, the same heat transfer coefficient determined for the 90 PRF mixture was used, and the same pressure-time history was used, corresponding to the critical compression ratio for RON of 90, as previously discussed. The computed times of autoignition for these fuels are summarized in Table IV, with the fuels listed in order of increasing value of RON. The ignition times are given in milliseconds, where zero time occurs at bottom dead center and 22° ATDC is equivalent to 58.0 milliseconds. With a few exceptions the overall correlation between RON and the computed time of ignition is quite good, and there are a number of high octane number fuels for which the model indicates no ignition at all during the engine cycle. On a very simple level, nearly all of the fuels with RON less than 90 are calculated to ignite before 58.0 ms.

Fuel		RON	Time of ignition (ms)
n-heptane	C_7H_{16}	0	55.0
n-hexane	C_6H_{14}	25	55.0
2-methyl hexane	C_7H_{16}	42	54.5
n-pentane	C_5H_{12}	62	55.9
3-ethyl pentane	C_7H_{16}	65	57.4
2-methyl pentane	C_6H_{14}	73	55.5
3-methyl pentane	C_6H_{14}	74	57.2
3,3-dimethyl pentane	C_7H_{16}	81	55.7
2,4-dimethyl pentane	C_7H_{16}	83	56.2
2,2-dimethyl propane	C_5H_{12}	86	56.4
2-methyl butane	C_5H_{12}	92	59.1
2,2-dimethyl butane	C_6H_{14}	92	59.9
2,2-dimethyl pentane	C_7H_{16}	93	*
n-butane	C_4H_{10}	94	57.6
2,3-dimethyl butane	C_6H_{14}	100	58.0
2,2,4-trimethyl pentane	C_8H_{18}	100	58.5
2-methyl propane	C_4H_{10}	102	*
propane	C_3H_8	112	*
2,2,3-trimethyl butane	C_7H_{16}	112	*
ethane	C_2H_6	115	*

* no ignition

Table IV

Computed times of ignition for selected alkane fuels using RON 90 pressure history

The same computed results are plotted in Fig. 2, with calculated time of ignition shown as a function of RON. Also in Fig. 2 is a solid curve drawn through the points for n-heptane, iso-octane, and the calibration point for 90 PRF at 58.0 ms. This curve represents a form of PRF calibration curve, and the two dashed curves have been drawn to indicate a band approximately 0.5 ms on either side of this calibration curve.

There are two major features of Fig. 2 that are of general importance. First, most of the computed results fall within ±0.5 ms of the central curve, and second, the shape of the curve indicates little change in computed time of ignition with RON for low octane fuels but a much more sensitive dependence as RON increases above approximately 80.

Examination of the computed results provides a great deal more kinetic information in addition to the predicted time of autoignition. In general, as the octane number increases, the amount of chemical activity at a given time tends to decrease and the chemical species concentrations which are observed tend to change. For example, if we examine each computed model at a time of 54 ms, which is later than TDC but still prior to ignition in all of the cases, we can use the OH radical concentration to compare each of the fuels. For all of the fuels examined, the OH concentration decreases steadily as the RON increases. In addition, the levels of peroxide species, of cyclic ethers and other indicators of RO_2 radical isomerization all increase as RON decreases, in all of the model calculations. Furthermore, the model calculations show clearly that the sequence of reactions

$$RO_2 \rightarrow QOOH \rightarrow \text{epoxide} + OH$$

provides a large percentage of the OH concentrations at all times prior to ignition, and the fraction of the total OH concentration provided through these paths increases steadily as the RON decreases.

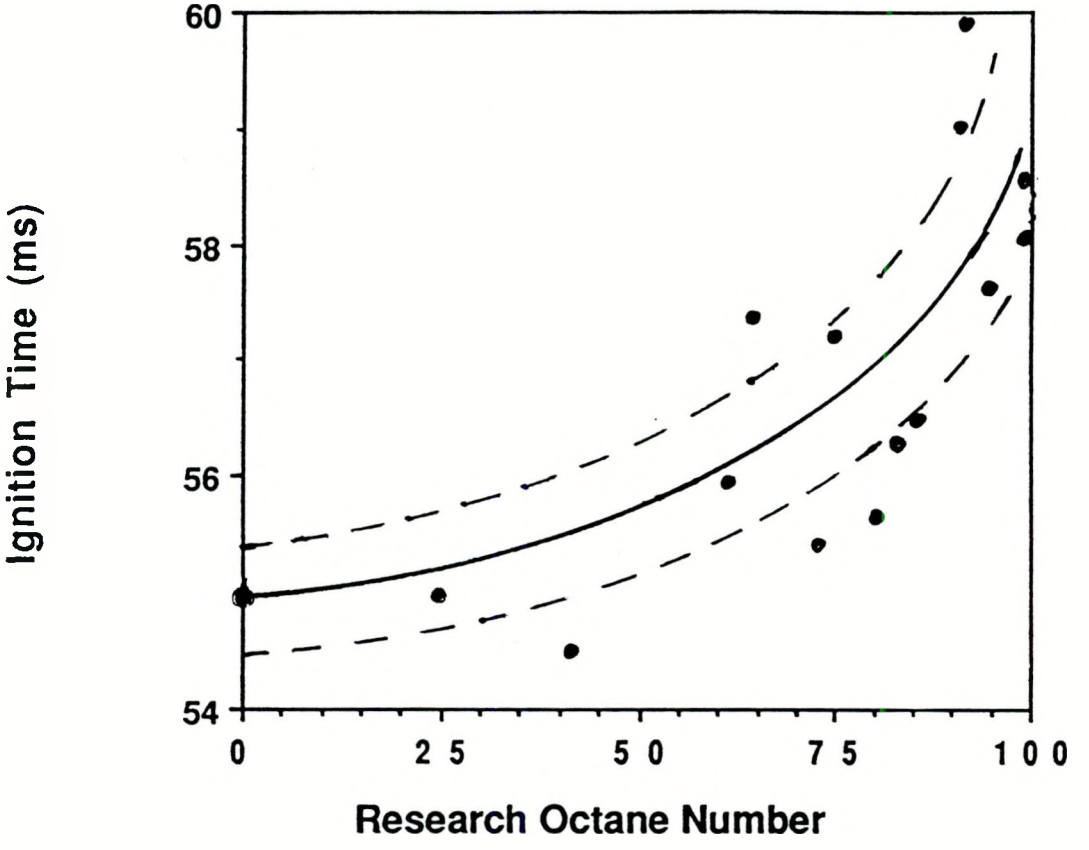

Figure 2

Computed times of autoignition for the C_2-C_6 fuels in Table IV, showing the correlation with Research Octane Number.

Sensitivity analysis of the computed results to the rates of different families of elementary reactions provides additional information about important reaction sequences. In each model calculation, we can vary the rates of each group of reactions and compute new times of ignition. Some rate changes increase the time of ignition while others reduce the time of ignition. Most reaction rate changes have relatively little effect on the time of ignition. The types of reactions which were found to have the greatest impact on the computed times of ignition are the equilibrium constants of the O_2 addition reactions

$$R + O_2 = RO_2 \quad ,$$

and the rates of RO_2 isomerization

$$RO_2 = QOOH \quad .$$

These RO_2 isomerization reactions contribute significantly to the rate of OH radical production, since the QOOH products decompose to produce cyclic ethers and OH radicals as discussed above. Another group of reactions whose rates have a significant impact on the computed results are those of the type

$$RH + HO_2 = R + H_2O_2 \quad , \text{ and}$$

$$RH + RO_2 = R + ROOH \quad .$$

Both of these families of reactions lead to OH production through the decompositions

$$H_2O_2 = OH + OH \quad , \text{ and}$$

$$ROOH = RO + OH \quad .$$

The decomposition of hydrogen peroxide has a relatively high activation energy and does not proceed rapidly until the end gas temperature reaches a temperature of 950 K or greater. However, the decomposition of QOOH species takes place at somewhat lower temperatures, and these reactions provide an appreciable fraction of the OH production in the end gases.

Another group of reactions with a significant impact on the computed model results consists of QOOH decompositions to produce HO_2

$$QOOH\ (\alpha) = Q + HO_2 \quad .$$

As indicated here, this alternate route is possible only for QOOH radicals where the internal H atom abstraction in RO_2 has taken place at the α site, immediately adjacent to the site of the O_2 addition. This path competes with the production of OH and an epoxide species. When we use the model to artificially increase the rate of the above HO_2 product path, the computed ignition times increase, so this path tends to inhibit or slow the ignition process. When the rate of the alternative product path leading to OH and an epoxide is increased, the computed ignition times become shorter. The sensitivity to this competition for these QOOH radicals is somewhat surprising, in view of the fact that internal H atom abstraction at the α-site is inhibited by a large ring strain energy barrier, but this indicates how important OH production can be to the overall ignition process.

Finally, computed results were dependent on the rate of addition of O_2 to QOOH radicals. Although the fraction of QOOH radicals which react via this path is relatively small, the production of so many radical species, including the two OH radicals, makes this still an important reaction type in our computations.

FUEL MIXTURES

Since real automotive fuels consist of mixtures of hydrocarbons, it is very important to be able to predict the ignition properties of such mixtures. In some cases the ignition properties of fuel mixtures can be quite complex and be much different from the average behavior of the components in the mixture. This is particularly true in cases where one relatively unreactive fuel is mixed with another which is considerably more reactive [25].

Recently, Croudace and Jessup [2] determined the octane ratings of many isomeric hexanes, including the neat fuels, all of the 50-50 binary combinations, all of the equal mixtures of four hexanes, and the mixture with 20% of each hexane. In most of these mixtures it was found that the mixture octane number was greater than that predicted by linear blending assumptions, although the opposite trend was observed for several of the mixtures. These results were interpreted qualitatively in terms of the same type of peroxy radical isomerization theory as used in the present study, in which we provide a numerical application of that approach. Their experimental study provided us with the suggestion to include these hexane mixtures in our modeling work.

We examined two mixtures, each consisting of two isomers of hexane. In both cases the relatively non-reactive fuel is 2,2-dimethyl butane, with its RON of 92, for which our model computed an ignition time of 59.9 ms (see Table IV). In the first case the second component was n-hexane, with RON of 25 and a computed time of ignition of 55.0 ms. We can use the solid curve in Fig. 2 to illustrate the results, where the computed results for both n-hexane and 2,2-dimethyl butane fall close to the solid

curve. A mixture of equal parts n-hexane and 2,2-dimethyl butane was found to ignite at a time of 56.4 ms, which translates in Fig. 2 into RON=70. This is significantly larger than the average RON for the two hexanes of 58.5. Our computed result is in excellent agreement with that measured by Croudace and Jessup [2], who observed a value of RON = 72 for this mixture and commented on the large degree of positive interaction between these two fuels. They also observed large positive interactions for all of the other hexane isomers when mixed with n-hexane, suggesting that the branched additive suppresses much of the cool flame alkylperoxy isomerization reactions that are so dominant in the n-hexane fuel mixture. In another computed result, a mixture of 75% n-hexane and 25% 2,2-dimethyl butane was found to ignite at 55.7 ms, corresponding to RON=43, while linear blending would predict RON=42, in good agreement with the computed value.

The second mixture of hexanes studied with the numerical model included an equimolar mixture of 2,2-dimethyl butane and 3-methyl pentane. 3-methyl pentane has a RON of 74 and a predicted time of ignition of 57.2 ms. This is an interesting mixture, first because both fuels have relatively high octane numbers, so the wide disparity in RON encountered in the previous example is avoided. Second, the computed time of ignition for 3-methyl pentane is slightly longer than would be predicted by the correlation in Fig. 2. The model results for these mixtures demonstrated two interesting trends. Addition of very small amounts of 3-methyl pentane to the other fuel rapidly degraded its knock resistance. For example, a mixture of 90% 2,2-dimethyl butane and 10% 3-methyl pentane was predicted to ignite at 57.4 ms, only slightly longer than the 57.2 ms predicted for 100% 3-methyl pentane. In addition,

the higher octane fuel actually accelerated ignition of the 3-methyl pentane. As a result, all mixtures of the two fuels with more than 20% 3-methyl pentane ignited more rapidly than either pure component fuel. Croudace and Jessup reported slightly antagonistic behavior for mixtures of these isomers; that is, values of RON for mixtures were observed to be somewhat less than would have been predicted from an assumption of linear blending, but they did not report any evidence of the RON of mixtures of these isomers being smaller than the RON of either pure component. Because the computed results for both fuels do not yet agree accurately with the correlation in Fig. 2, it is likely that the reaction mechanisms for these fuels are still not completely correct. As these reaction mechanisms are improved, predicted behavior of mixtures should also be expected to behave in a more realistic manner.

It is not the intent of the present study to examine exhaustively the behavior of binary mixtures of fuels, but rather to demonstrate the performance of the current kinetic model in simulating the ignition of fuel mixtures having different ignition characteristics. The results already presented indicate that in cases where the model correctly predicts the ignition behavior of both components, mixtures of these components can be treated in a reasonably quantitative fashion. In cases such as the mixture of 2,2-dimethyl butane and 3-methyl pentane, where one of the fuels is not yet properly described, the model can reproduce some of the observed trends but cannot provide quantitative predictions.

Primary Reference Fuels

Another independent series of mixture calculations that we carried out some time ago [7] included mixtures of n-heptane and iso-octane. Using the same reaction mechanisms as used for the hexanes, the ignition times for mixtures ranging from 100% iso-octane (RON = 100) to 100% n-heptane (RON = 0) were computed. The results of the model calculations are shown graphically in Fig. 3. The solid curve shows the computed temperature history from the input pressure history with no heat release due to reactions. The other curves show the computed temperatures for the indicated PRF mixtures, showing a clearly monotonic variation in computed ignition time with the mixture value of RON. The same results can be shown on the same basis as illustrated earlier in Fig. 2, indicating computed time of ignition and its correlation with RON. These PRF results are shown in Fig. 4 for PRF mixtures of RON 0 (i.e. n-heptane), RON 100 (iso-octane), and the mixtures for RON 50 and RON 90. As shown in Fig. 4, the computed ignition times correlate very closely with the same trends determined previously for the pentanes, hexane, and heptanes.

KNOCK INFLUENCE OF ADDITIVE COMPOUNDS

In the previous section, kinetic modeling of fuel mixtures was described. It was implicit in our discussion that each of the fuel components was a primary fuel itself and that we were concerned primarily with blending properties. However, another logically distinct class of problems is concerned with the use of rather small amounts of additive species which can have a disproportionate effect on the ignition of a primary fuel. These additives can either promote or inhibit ignition, depending on the details of their kinetic interaction with the ignition of the primary fuel. In the following sections we report numerical results for both types of additives.

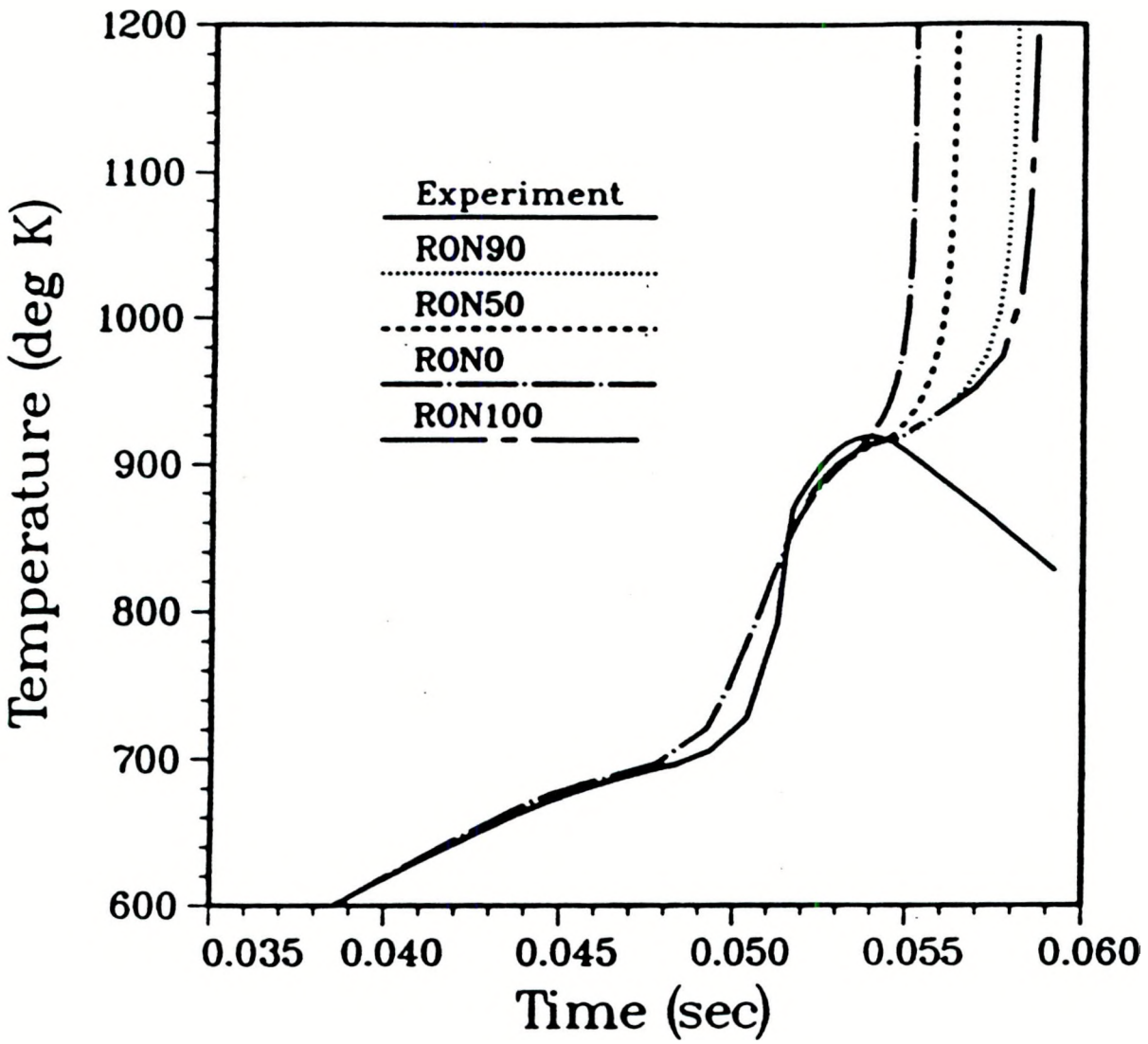

Figure 3

End-gas temperatures for PRF mixtures
The solid curve indicates temperature computed from the experimentally measured pressure, using a thermodynamic model, and the other curves show model computations with the indicated n-heptane/iso-octane mixtures.

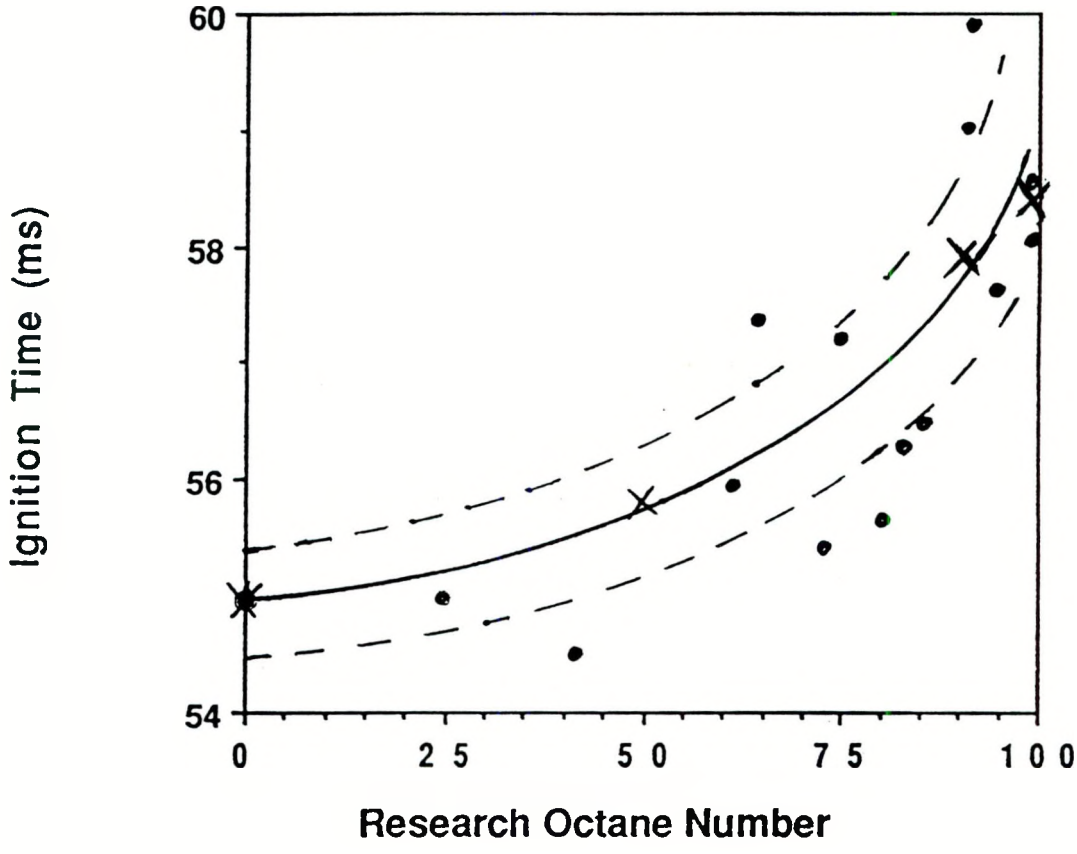

Figure 4

Computed times of autoignition for PRF mixtures
The X symbols indicate model results for RON=0, 50, 90, and 100.
The remaining filled symbols are the same as in Fig. 2.

The most important qualification for inclusion in our study is that a tested kinetic reaction mechanism be available for the oxidation reactions of the additive species. In many cases the reaction mechanisms for these additives are already included as submechanisms in the hexane and heptane mechanisms. We developed additional reaction mechanisms for other additives, including t-butyl peroxide, azo-t-butane, dimethyl ether, methyl tert-butyl ether (MTBE), and ethyl tert-butyl ether (ETBE). In the cases of MTBE and ETBE, we have recently [26] reported a detailed kinetic study of the ignition of mixtures of propane/MTBE and propane/ETBE in shock tubes. These reaction mechanisms have been taken directly from those shock tube studies and used without further modification in the present work.

Pro-knock Additives

A wide range of additives were found to decrease the ignition time of the primary fuels. Listed below are the species added to different hexane isomers which were considered.

acetone	CH_3COCH_3
t-butyl hydroperoxide	tC_4H_9OOH
p-butyl hydroperoxide	pC_4H_9OOH
s-butyl hydroperoxide	sC_4H_9OOH
methyl hydroperoxide	CH_3OOH
hexyl hydroperoxide	$C_6H_{13}OOH$
methanol	CH_3OH
1-butene	$1C_4H_8$
hexene	C_6H_{12}
acetaldehyde	CH_3CHO
hydrogen peroxide	H_2O_2
t-butyl peroxide	$tC_4H_9OOC_4H_9t$
azo-t-butane	$tC_4H_9NNC_4H_9t$
dimethyl ether	CH_3OCH_3

In the above list, several of the compounds are incompletely specified, such as 'hexene' and 'hexyl hydroperoxide'. For simplicity, these species were selected from the list of hexenes or hexyl hydroperoxides already present in each hexane reaction mechanism. This permitted us to assess the impact of this type of species without unnecessarily adding to the complexity of the reaction mechanism. For the sake of illustration, we will discuss the computed results for which the primary fuel was 2,2-dimethyl butane. This fuel has a relatively high octane number (92) with a computed time of ignition is late (59.9 ms), and the computed results for its additives were representative of all of the results we obtained with other hexane isomers.

Little or no change was observed in the time of ignition when the additive was acetone, hexene, acetaldehyde, or methanol. Modest decreases in the time of ignition were computed when the additive was butene or hydrogen peroxide. Dramatic decreases in ignition time were observed for all of the hydroperoxides, t-butyl peroxide, and azo-t-butane.

For a fixed amount of additive, amounting to only 0.01% of the fuel, the following additives reduced the time of ignition for 2,2-dimethyl butane from its initial value of 59.9 ms.

Additive	Ignition (ms)
azo-t-butane	54.8
t-butyl peroxide	55.0
p-butyl hydroperoxide	55.1
hexyl hydroperoxide	55.3
methyl hydroperoxide	55.4
s-butyl hydroperoxide	55.4
t-butyl hydroperoxide	55.4
H_2O_2	57.0
1-butene	58.7

All of the additives which have an appreciable effect on the rate of ignition act by providing radical species, particularly OH radicals, in

significant quantities at earlier times and in amounts that are greater than ordinarily produced by the primary fuel. This excess supply of radicals accelerates the overall rate of ignition and results in an earlier time of ignition and lower effective octane rating. The reaction

$$ROOH = RO + OH$$

provides OH radicals at temperatures between 800 and 900 K, which are reached by the end gases at times before TDC. Ordinarily, without an additive, the reactive gas must produce its own hydroperoxide species and their product OH radicals, and this is difficult to achieve in the quantities which are available from decomposition of the ROOH additives.

The sensitivity of the computed results to the amounts of additives are greater than experimental evidence would suggest. The addition of only 0.01% of one of these hydroperoxide species effectively decreases the RON for 2,2-dimethyl butane from 92 to a value between 0 and 30. This is a greater sensitivity than would be expected experimentally. However, the model indicates that the greatest fraction of the additive dissociates rather abruptly when the temperature reaches a critical value, and at a concentration of 0.01% of the fuel, this is an extremely large value for a sudden pulse of radical species, especially one as reactive as OH.

Over the years there has been a great deal of debate concerning whether aldehydes or hydroperoxides are the most important branching agents leading to engine knock. The present additive calculations, in which aldehyde addition has virtually no effect on octane number but hydroperoxides are very effective in promoting knock, suggest strongly that hydroperoxides are important through their production of OH at the times when they are most effective in expediting ignition.

Anti-knock additives

Perhaps the most important additives to be considered are those that increase the effective octane number of a given hydrocarbon fuel. In previous numerical studies [5] we demonstrated how tetraethyl lead (TEL) acts by catalytically removing active radicals, especially HO_2, from the radical pool and suppressing the high temperature ignition of the fuel. Together with our current study, it is apparent that there are several distinct ways in which an anti-knock species can influence ignition.

At relatively low temperatures, an additive can interfere with the alkylperoxy isomerization reaction paths which precondition the fuel-air mixture and consume small amounts of the fuel. The additive can also inhibit the higher temperature ignition that is driven by the conversion of HO_2 to H_2O_2 and then to OH. Our present study indicates that one class of additives, including MTBE and ETBE, are particularly effective because they act over both temperature ranges.

We developed a detailed kinetic reaction mechanism to describe the reactions of MTBE and ETBE. These reactions include the thermal decomposition of the additive, H atom abstraction from each site in the molecule, and ß-scission of the resulting radicals into smaller fragments. Internal H atom abstraction within the radical species is also included. Many of the elementary reaction rate exppressions have been taken from the work of Brocard et al. [27]. In addition, site-specific H atom abstraction reaction rates were estimated using the same techniques as those described earlier to provide site-specific rate data in large hydrocarbon fuel species. Brocard et al. noted that RO_2 reaction paths were unlikely to be significant for most experimental conditions, and these steps were not included in our current modeling work.

We can illustrate our computed results with MTBE added to several of the hexane fuels. We will compare our computed results with experimentally determined results obtained by Leppard [28], who observed a wide variety of intermediate species produced during the ignition of fuel/MTBE mixtures.

The fuels considered in our computations were nC_6H_{14}, with RON of 25 and a computed time of ignition at 55 ms, 2-methyl pentane (73, 55.5 ms), 3-methyl pentane (74, 57.2 ms), and 2,3-dimethyl butane (100, 58.0 ms). We replaced fractions of the hexane fuels with corresponding amounts of MTBE and computed the new time of ignition, relating the result to an effective value of the octane number. The computed results for mixtures with various amounts of the total fuel consisting of MTBE are summarized in Table V. For each of the fuels, we have indicated in the last column the value of RON that corresponds to the value in Fig. 2 for the computed ignition time, rather than the actual RON value for that fuel.

The computed results show that the increase in computed RON value is proportional to the percentage of MTBE in the mixture. The increase in RON per amount of MTBE added is not the same for each hexane fuel, but in each case the effect is qualitatively the same. In Fig. 5 we have indicated the computed times of ignition for the n-hexane/MTBE mixtures, and it is very clear that the RON increment for each 5% of MTBE added is close to 23 and is effectively constant over the entire range studied. It is important to note that the mixture values of RON are significantly greater than would be predicted from an assumption of linear blending of the two components. The same observation is true for the other hexane isomers.

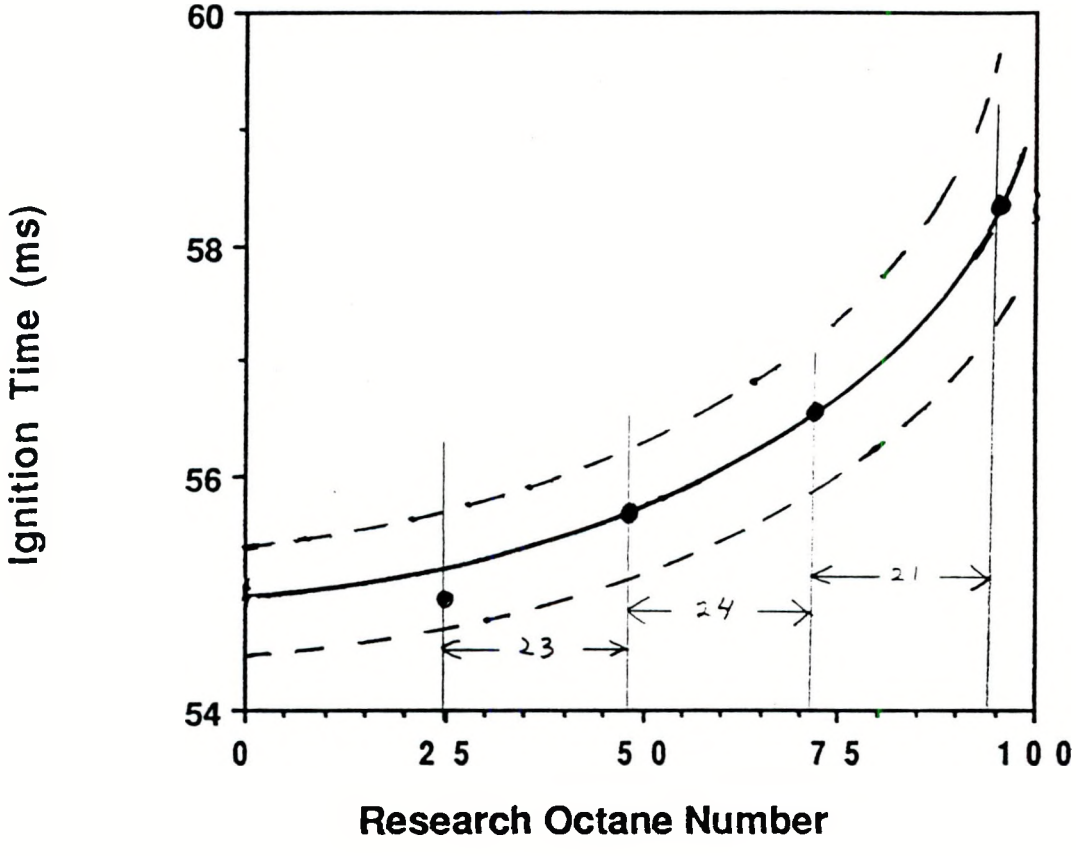

Figure 5

Computed times of autoignition for mixtures of n-hexane and MTBE
The fuel mixtures are listed at the beginning of Table V.
The resulting predictions of mixture RON and the increments
as MTBE is added are also shown.

n-hexane	MTBE	Ignition (ms)	RON (effective)
1.0	0.	55.0	25
0.95	0.05	55.7	48
0.90	0.10	56.5	72
0.85	0.15	58.4	93
2-methyl pentane			
1.0	0.	55.5	45
0.9	0.10	56.5	70
0.85	0.15	57.4	85
0.80	0.20	59.2	100
3-methyl pentane			
1.0	0.	57.3	88
0.95	0.05	58.6	96
2,3-dimethyl butane			
1.0	0.	57.4	84
0.95	0.05	58.3	94
0.90	0.10	60.9	105
2,3-dimethyl butane at 20° elevated temperature			
1.0	0.0	54.8	0*
0.9	0.1	54.9	20*
0.75	0.25	55.7	50*
0.5	0.5	59.0	98*

* values taken from Fig. 1, not intended as actual RON values

Table V

Ignition of hexane isomers with mtbe additive

For the other hexane isomers, we must consider the fact that the predicted time of ignition for the pure hexane fuel is not exactly in agreement with the solid curve in Fig. 2. However, if we use the RON that corresponds to the value related to the ignition time actually computed for each fuel, a linear variation in mixture RON is again predicted. Another series of computed ignition calculations was carried out with 2,3-dimethyl butane as the fuel but with a somewhat higher initial temperature than in the previous calculations. The initial temperatures in this series of calculations were 20K higher than in all of the other calculations, so all of the ignition times are earlier than in the previous series. However, the inhibition of ignition, as shown in Table V, is again still quite linear and more rapid than would have been predicted on the basis of linear blending.

Leppard [28] has measured the concentrations of virtually all of the intermediate species produced during the pre-ignition period of the entire range of 2,3-dimethyl butane mixtures with MTBE. This information can provide important confirmation about our kinetic model for ignition. The current model confirms the observations and provides insight into why MTBE is such an effective anti-knock additive.

Leppard indicates that when used as a fuel itself, MTBE exhibits no intermediate products of RO_2 isomerization, and this is confirmed by the model calculations. For mixtures with both 2,3-dimethyl butane and MTBE, the only major cyclic ether species observed experimentally is 2,2,3-trimethyl oxetane, which is also the dominant cyclic ether predicted by the model. Generally speaking, the same ranking of intermediate species observed experimentally is reproduced closely by the model calculations. It is interesting to note from the experiments that the principal large olefins are 3-methyl-1-butene and 2-methyl-2-butene,

rather than C_6 olefins. These species are produced by RO_2 isomerization reactions with the H atom abstracted from the ß-site. However, these olefins are present in amounts that are quite small compared with acetone and propene, both of which are produced by a sequence of reactions beginning with abstraction of tertiary H atoms in the fuel, followed by O_2 addition at the tertiary site. Internal abstraction of the remaining tertiary H atom leads to production of acetone and propene in roughly equal amounts. Internal abstraction of H atoms at the most distant primary site leads to the observed oxetan products, and the ratio of the two groups of products provides us with extremely useful data concerning the relative rates of internal H atom abstraction.

There are three separate factors involving MTBE (and ETBE) which appear to be important in determining its anti-knock effectiveness. First, it possesses a significant number of H atoms (12 in the case of MTBE) which consume radical species, especially OH, during the lower temperature phase of the ignition period. The importance of this process was confirmed by the numerical model by artificially modifying the rates of OH reacting with MTBE. When these abstraction rates were decreased, the model predicted that mtbe was less effective in inhibiting ignition, and when these rates were increased, the ignition time was even further delayed. The same numerical experiment was carried out for reactions between MTBE and the HO_2 radical. In direct contrast with the results for OH, increasing the rate of MTBE+HO_2 reactions made the MTBE less effective as an anti-knock additive, since the additional H_2O_2 produced by such a path then decomposed into OH+OH, accelerating the ignition process. This series of calculations demonstrates very clearly

that it is the impact on the OH radical population that is especially important in retarding knock. This also is consistent with the strong pro-knock effects of the alkyl hydroperoxide species discussed above, which we noted were effective because they added excess OH radicals to the radical pool during the preignition period.

The second factor responsible for the behavior of MTBE has already been noted, the fact that MTBE does not participate in any appreciable amount of cool-flame activity. Although O_2 addition to MTBE radicals will certainly occur, the resulting RO_2 radicals do not readily abstract other H atoms from within the radical species. This fact is confirmed by the experimental observations of Leppard [28] and must be due to the existence of only primary C - H bonds in the molecule and the presence of the additional O atom in the ether radical. Because RO_2 isomerizations are not observed for MTBE, it does not produce excess OH radicals via such reaction paths. By displacing other fuel species which do produce OH by such reaction paths, addition of MTBE reduces the overall production of OH at these lower temperatures.

Finally, the major product of MTBE reaction is iso-butene, a species which provides its own complex network of chemical interactions with the ignition process. Iso-butene itself, both experimentally and in our knock calculations, is much less effective than MTBE in influencing autoignition under engine conditions. However, under higher temperature conditions such as those in shock tubes, we have found that MTBE and iso-butene are equally effective in inhibiting ignition [26]. At these higher temperatures, RO_2 kinetics are completely unimportant, and these species act by consuming radical species and producing unreactive intermediate

species. In our engine ignition model, the iso-butene acts primarily during the higher temperature ignition phase itself when the dominant radical species is HO_2. This is the same regime in which TEL inhibits ignition; iso-butene is less effective than TEL in retarding this ignition process between 900K and 1000K, but even a small impact on the radical pool at this time will slow the ignition to some degree.

As a result, it appears that MTBE is a very effective anti-knock additive because it retards radical pool growth and chain branching in both the low temperature cool flame regime and the higher temperature explosion regime, combined with the fact that it does not provide excess radical species during its own ignition.

The same arguments can be made for the case of ETBE as well. The ETBE is even more effective in removing OH from the reaction in the low temperature regime, since it possesses two additional secondary H atoms. After one of those secondary H atoms is abstracted, all sites available for internal H atom abstraction are inhibited just as in the case of MTBE. However, initial abstraction of primary H atoms from the ethyl end of ETBE can lead to some RO_2 isomerization through internal abstraction at the secondary sites.

Leppard [28] also studied the effects of addition of tertiary amyl methyl ether (TAME), which is somewhat less effective than MTBE or ETBE as an anti-knock additive. We did not carry out modeling calculations for TAME as the additive, but the concepts developed above can still be used to analyze its effects during ignition. In the case of TAME, the significantly larger alkyl radical on one side of the O atom permits much more RO_2 isomerization activity to occur than in the cases of MTBE and

ETBE. This leads to production of OH radicals, in part defeating the effects of OH removal through reaction with the TAME itself. In addition, the products of TAME reaction will not be dominated by iso-butene, and the inhibiting qualities of these products may not be as significant as those of iso-butene.

The present model is constantly being refined and corrected as new information becomes available from engine experiments, pure kinetics experiments, and theoretical analyses. We have identified many of the parts of the mechanisms where improvement is needed, particularly those areas where the computed results are sensitive to kinetic assumptions that have little experimental data for support. However, even in its present form, the model provides a great deal of insight and quantitative information regarding the chemical reactions leading to engine knock.

CONCLUSIONS

The present kinetic model provides a useful tool to examine and understand a great deal of experimental information about the behavior of octane number in complex fuel systems. While not yet completely refined to the point where all available octane number data can be completely interpreted, the model represents an important step towards the eventual goal of being able to predict the knock sensitivity of complex mixtures of fuels, additives, and other constituents and the development of fuels with any desired octane rating.

In particular, these modeling results demonstrate the extreme importance of RO_2 isomerization processes in explaining knock sensitivity. The OH radicals produced by such reaction paths consume some of the fuel, which accelerates ignition, but more important, they produce

a radical pool and a reactive mixture which is then more rapidly ignited as the end gas temperature reaches about 900K.

This behavior explains the widely observed trends that long chain hydrocarbons have low octane numbers and knock easily while highly branched fuels are knock-resistant. The present model shows that compact, highly branched fuels have high knock resistance for two simple reasons. First, the majority of the available H atoms are located at primary sites and are therefore relatively difficult to abstract, and second, the compactness of the molecule means that RO_2 isomerizations must overcome large ring strain energy barriers. Longer, straight-chain hydrocarbons incur neither energy barrier to RO_2 isomerization and therefore produce OH radicals from QOOH decomposition at much greater rates than in more compact, branched molecules.

The effectiveness of fuel additives as both pro-knock and anti-knock agents is also explained in terms of their impact on the OH radical pool. Additives which increase OH production accelerate ignition and promote knock, while additives which remove OH inhibit knock.

Anti-knocks can act either by retarding low temperature oxidation and chain branching or by inhibiting the higher temperature HO_2-dominated ignition. The additives MTBE and ETBE are effective anti-knocks in large part because they act in both the low temperature and the ignition regimes.

Work performed under the auspices of the U.S. Department of Energy by the Lawrence Livermore National Laboratory under contract number W-7405-ENG-48.

ACKNOWLEDGMENTS

The authors are pleased to acknowledge extensive interactions and discussions with Drs. R. M. Green of Sandia National Laboratories, M. C. Croudace and P. J. Jessup of Unocal, Profs. F. L. Dryer of Princeton University, N. P. Cernansky of Drexel University, and many others. We also appreciate the editorial reading of the original manuscript by Dr. Joseph Colucci of General Motors Research Laboratories.

References

1. Lovell, W. G., "Knocking Characteristics of Hysrocarbons," Ind. Eng. Chem. 40, 2388 (1948).

2. Croudace, M. C., and Jessup, P. J., "Studies of Octane Properties of Mixtures of Isomeric Hexanes," SAE paper SAE-881604, International Fuels and Lubricants Meeting and Exposition, Portland, Oregon (1988).

3. Westbrook, C. K., and Dryer, F. L., "Chemical Kinetic Modeling of Hydrocarbon Combustion," Prog. Energy Combust. Sci. 10, 1 (1984).

4. Westbrook, C. K., and Dryer, F. L., "Chemical Kinetics and Modeling of Combustion Processes," Eighteenth Symposium (International) on Combustion, p. 749, The Combustion Institute, Pittsburgh, 1981.

5. Westbrook, C. K., Pitz, W. J., Thornton, M. M., and Malte, P. C., "A Kinetic Modeling Study of n-Pentane Oxidation in a Well-Stirred Reactor," Combust. Flame 72, 45 (1988).

6. Westbrook, C. K., Dryer, F. L., and Schug, K. P., "A Comprehensive Mechanism for the Pyrolysis and Oxidation of Ethylene," Nineteenth Symposium (International) on Combustion, p. 153, The Combustion Institute, Pittsburgh, 1982.

7. Pitz, W. J., and Westbrook, C. K., "Chemical Kinetics of the High Pressure Oxidation of n-Butane and its Relation to Engine Knock," Combust. Flame 63, 113 (1986).

8. Kaiser, E. W., Westbrook, C. K., and Pitz, W. J., "Acetaldehyde Oxidation in the Negative Temperature Coefficient Regime: Experimental and Modeling Results," Int. J. Chem. Kinetics 18, 655 (1986).

9. Westbrook, C. K., Warnatz, J., and Pitz, W. J., "A Detailed Chemical Kinetic Reaction Mechanism for the Oxidation of iso-Octane and n-Heptane over an Extended Temperature Range and its Application to Analysis of Engine Knock," Twenty-Second Symposium (International) on Combustion, p. 893, The Combustion Institute, Pittsburgh, 1988.

10. Pitz, W. J., Westbrook, C. K., Proscia, W. M., and Dryer, F. L., "A Comprehensive Chemical Kinetic Reaction Mechanism for the Oxidation of n-Butane," Twentieth Symposium (International) on Combustion, p. 831, The Combustion Institute, Pittsburgh, 1984.

11. Cernansky, N. P., Green, R. M., Pitz, W. J., and Westbrook, C. K., "Chemistry of Fuel Oxidation Preceding End-Gas Autoignition," Combust. Sci. Technol. 50, 3 (1986).

12. Axelsson, E. I., Brezinsky, K., Dryer, F. L., Pitz, W. J., and Westbrook, C. K., "Chemical Kinetic Modeling of the Oxidation of Large Alkane Fuels: n-Octane and iso-Octane," Twenty-First Symposium (International) on Combustion, p. 783, The Combustion Institute, Pittsburgh, 1986.

13. Leppard, W. R., "A Detailed Chemical Kinetcs Simulation of Engine Knock," Combust. Sci. Technol. 43, 1 (1985).

14. Westbrook, C. K., and Pitz, W. J., "Detailed Kinetic Modeling of Autoignition Chemistry," SAE Trans. 7 96, 559 (1988).

15. Westbrook, C. K., and Pitz, W. J., "Modeling of Knock in Spark-Ignition Engines," International Symposium COMODIA 90: 11 (1990).

16. Benson, S. W., "The Kinetics and Thermochemistry of Chemical Oxidation with Application to Combustion and Flames,", Prog. Energy Combust. Sci. 7, 125 (1981).

17. Wagner, A. F., Slagle, I. R., Sarzynski, D., and Gutman, D., "Experimental and Theoretical Studies of the $C_2H_5 + O_2$ Reaction Kinetics," J. Phys. Chem. 94, 1853 (1990).

18. Baldwin, R. R., Dean, C. E., and Walker, R. W., "Relative Rate Study of the Addition of HO_2 Radicals to C_2H_4 and C_3H_6," J. Chem. Soc. Faraday Trans. 2, 82, 1445 (1986).

19. McAdam, K. G., and Walker, R. W., "Arrhenius Parameters for the Reaction $C_2H_5 + O_2 = C_2H_4 + HO_2$," J. Chem. Soc. Faraday Trans. 2, 83, 1509 (1987).

20. Bozzelli, J. W., and Dean, A. M., "Chemical Activation Analysis of the Reaction of C_2H_5 with O_2," J. Phys. Chem. 94, 3313 (1990).

21. Barnard, J. A., and Harwood, B. A., "Slow Combustion and Cool-Flame Behavior of iso-Octane," Combust. Flame 21, 345 (1973).

22. Barnard, J. A., and Harwood, B. A., "The Spontaneous Combustion of n-Heptane," Combust. Flame 21, 141 (1973).

23. Pollard, R. T., Hydrocarbons, Ch. 2, Comprehensive Chemical Kinetics, vol. 17, Gas-Phase Combustion (C. H. Bamford and C. F. H. Tipper, eds.), Elsevier, New York (1977).

24. Lund, C. M., "HCT - A General Computer Program for Calculating Time-Dependent Phenomena Involving One-Dimensional Hydrodynamics, Transport, and Detailed Chemical Kinetics," Lawrence Livermore National Laboratory report UCRL-52504 (1978).

25. Westbrook, C. K., "An Analytical Study of the Shock Tube Ignition of Mixtures of Methane and Ethane," Combust. Sci. Technol. 20, 5 (1979).

26. Gray, J. , and Westbrook, C. K., "Shock Tube Ignition of Mixtures of Propane and MTBE," Western States Section Meeting of The Combustion Institute, March 1991.

27. Brocard, J. C., Baronnet, F., and O'Neal, H. E., "Chemical Kinetics of the Oxidation of Methyl Tert-Butyl Ether (MTBE)," Combust. Flame 52, 25 (1983).

28. Leppard, W. M., "The Autoignition Chemistry of Octane-Enhancing Ethers and Cyclic Ethers: A Motored Engine Study," SAE paper SAE-91xxxx, International Fuels and Lubricants Meeting and Exposition, Toronto, Canada (1991).

Technical Information Department · Lawrence Livermore National Laboratory
University of California · Livermore, California 94551